Materials Research Bulletin 70 (2015) 397–402

Contents lists available at ScienceDirect

Materials Research Bulletin

journal homepage: www.elsevier.com/locate/matresbu

Solution combustion synthesis and enhanced electrochemical performance $Li_{1.2}Ni_{0.2}Mn_{0.6}O_2$ nanoparticles by controlling NO_3^-/CH_3COO^- ratio of the precursors

Qingtang Zhang [a,*], Juntao Mei [a], Xiaolong Xie [a], Xiaomei Wang [a,**], Junyan Zhang [b]

[a] State Key Laboratory of Advanced Processing and Recycling of Non-ferrous Metals, School of Petrochemical Engineering, Lanzhou University of Technology, Lanzhou 730050, China
[b] Lanzhou Institute of Chemical Physics, Chinese Academy of Science, Lanzhou 730000,China

ARTICLE INFO

Article history:
Received 17 October 2014
Received in revised form 30 April 2015
Accepted 2 May 2015
Available online 5 May 2015

Keywords:
A. Layered compounds
B. Sol–gel chemistry
C. Electrochemical measurements
D. Electrochemical properties
D. Energy storage

ABSTRACT

Lithium-rich layer oxide $Li_{1.2}Ni_{0.2}Mn_{0.6}O_2$ nanoparticles were fabricated through solution combustion synthesis by controlling NO_3^-/CH_3COO^- ratio of the precursors. The relationships between the NO_3^-/CH_3COO^- ratio and structure as well as electrochemical performance of $Li_{1.2}Ni_{0.2}Mn_{0.6}O_2$ nanoparticles are investigated. XRD reveals that $Li_{1.2}Ni_{0.2}Mn_{0.6}O_2$ nanoparticles obtained with a suitable NO_3^-/CH_3COO^- ratio of 3:1 (LLO-3N1A) is composed of the smallest nanocrystallite of 18 nm. SEM reflects that the average primary particles of LLO-3N1A are the smallest with a size of 35 nm. Those unique characteristic guarantee the excellent electrochemical performance of LLO-3N1A. LLO-3N1A exhibits a specific capacity of 252.3 mA h g^{-1} at 0.1 C. In addition, LLO-3N1A also shows best rate capability among the four prepared $Li_{1.2}Ni_{0.2}Mn_{0.6}O_2$ samples.

1. Introduction

With the excellent performance such as high power density, high energy density, long cycling life and environmental benignity [1–3], lithium ion batteries (LIB) have been expanded to a wide range of applications beyond the portable power source like hybrid electric vehicles, plug-in hybrid electric vehicles and electric vehicles, etc. The development of high-energy LIB extremely demands cathode materials with high specific capacity to match the anode materials [2,4–6], which possess a high specific capacity larger than 340 mA h g^{-1}. However, conventional cathode materials such as $LiCoO_2$ [7], $LiNi_{1/3}Co_{1/3}Mn_{1/3}O_2$ [8], $LiFePO_4$ [9] and $LiMn_2O_4$ [10] only deliver a specific capacity lower than 180 mA h g^{-1}. Therefore, lithium-rich layered oxides based on $xLi_2MnO_3{\cdot}(1\text{-}x)\ LiMO_2$ (M = Co, Ni, Mn, etc.), are undoubtedly becoming appealing as cathode materials for high-energy LIBs due to their high capacity (>200 mA h g^{-1}) [11–15].

Despite the outstanding advantages of lithium-rich layered oxides, these materials are plagued with problems like large initial irreversible capacity [11–13] and capacity decay during charge–discharge cycles [11,16]. In addition, the achievement of high-rate capability is hindered by the kinetic barriers such as intrinsic poor electronic conductivity and low lithium-ion diffusion because the flow of electrons and diffusion of lithium-ions in the lithium-rich layered oxides are blocked by the occupancy of the excess lithium-ions in the transition metal layer [13–17]. Some efforts have been tried to solve these problems. For instance, surface nitridation [16] or coating with oxides [11,18–22], fluorides [23,24], phosphates [25,26] and carbon [27,28] are proved to be effective to improve the electrochemical performance of lithium-rich layered oxides. In addition, fabrication of cathode material with reduced particle size is also demonstrated to improve the high-rate capability of lithium-rich layered oxides [29–35]. However, the above lithium-rich layered oxides with a primary particle size of 100–300 nm are relatively large. Thus, it is necessary to investigate the electrochemical performance of lithium-rich layered oxides with a more reduced primary particle size.

Among those lithium-rich layered oxides, cobalt-free $Li_{1.2}Ni_{0.2}Mn_{0.6}O_2$ (also designated as $0.5Li_2MnO_3{\cdot}0.5LiNi_{0.5}Mn_{0.5}O_2$) attracted much attentions due to its low cost, eco-friendly and comparatively good electrochemical performance. Many efforts have been done to investigate the structure and electrochemical performance of $Li_{1.2}Ni_{0.2}Mn_{0.6}O_2$ [11,16,24, 26–28,30–44]. However, combustion method was seldom used to prepare $Li_{1.2}Ni_{0.2}Mn_{0.6}O_2$ [44]. As a matter of fact, combustion method is very conventional in fabricating other cathode materials like $LiMn_2O_4$ with reduced particle size [10,45–47]. In the previous

---

* Corresponding author. Tel.: +86 931 7823127; fax: +86 931 7823001.
** Corresponding authors.
E-mail addresses: zhqt137@163.com (Q. Zhang), wxmei06@163.com (X. Wang).

http://dx.doi.org/10.1016/j.materresbull.2015.05.005
0025-5408/© 2015 Elsevier Ltd. All rights reserved.

study [10], we successfully investigated the effect of NO_3^-/CH_3COO^- ratio on the structure and electrochemical performance of micro-sized $LiMn_2O_4$. Obviously, Mn valence in $Li_{1.2}Ni_{0.2}Mn_{0.6}O_2$ (+4) is quite different from the Mn valence in $LiMn_2O_4$ (+3.5). Therefore, the NO_3^-/CH_3COO^- ratio will play different role on the structure, morphology and electrochemical performance of $Li_{1.2}Ni_{0.2}Mn_{0.6}O_2$. Here, we aim to prepare $Li_{1.2}Ni_{0.2}Mn_{0.6}O_2$ nanoparticles via solution combustion synthesis by simply controlling NO_3^-/CH_3COO^- ratio. In addition, the structure, morphology and electrochemical performance of $Li_{1.2}Ni_{0.2}Mn_{0.6}O_2$ nanoparticles will also be investigated.

2. Experimental

2.1. Preparation of samples

In order to control the NO_3^-/CH_3COO^- rate, five salts such as $LiNO_3$ (Aladdin, Shanghai), $Ni(NO_3)_2·6H_2O$ (Aladdin, Shanghai), $Ni(CH_3COO)_2·4H_2O$ (Aladdin, Shanghai), $Mn(CH_3COO)_2·4H_2O$ (Aladdin, Shanghai) and 50 % $Mn(NO_3)_2$ solution (Kaixin, Tianjin) were used as the starting materials. All the chemicals are analytical grade. Four typical samples were prepared and they are defined as LLO-1N1A, LLO-3N1A, LLO-4N1A and LLO-N, respectively. The amounts of raw materials used to prepare the four samples are illustrated in Table 1 (The number 0.000 means that amount of the salt is zero). The synthesis procedure is described as follows. Firstly, different amounts of raw materials were dissolved into ethanol in a 200 ml porcelain evaporating dish. Secondly, the solutions were evaporated at 80 °C under constant stirring to obtain the gels. Thirdly, the gels were auto-ignited combusted above 250 °C to get the fluffy precursor, and the precursor was then grinded in an agate mortar. Finally, the grinded precursors were calcinated at 700 °C for 10 h in an air filled muffle furnace and then took out immediately in order to cool them quickly to the room temperature.

2.2. Characterization

The crystalline structure of the four as prepared samples was determined by X-ray diffraction (XRD) using a Rigaku RINT2000 X-ray diffractometer over with Cu Kα radiation ($\lambda = 0.154$ nm). The scanning angle 2θ was scanned in the range of 10–90° with a rate of 4° (2θ) min^{-1}. The microstructure of the four samples was then investigated by a scanning electron microscopy (SEM, JSM-6700F).

80 wt.% prepared $Li_{1.2}Ni_{0.2}Mn_{0.6}O_2$ samples were homogeneously mingled with 10 wt.% Super P carbon black and 10 wt.% aqueous LA132 binder (Chengdu Indigo Power Sources Co., Ltd.) in an agate mortar to prepare the viscous slurry. Then, the slurry was coated on a 20 μm aluminum foil and split to 12 mm circular disks (composite cathode). Subsequently, the composite cathode was dried in a vacuum drying oven at 100 °C for 8 h and then weighed. Coin-type CR2032 cells were assembled by using the weighed composite cathode, lithium flake anode, Celgard 2400 separator and electrolyte in an argon-filled glove box. The electrolyte is 1 mol/L $LiPF_6$ dissolved in a mixture of ethylene carbonate/dimethyl carbonate/ethyl–methyl carbonate (EC/DMC/EMC is in a volume ratio of 1:1:1), which is provided by Shenzhen Capchem Chemicals.

Table 1
The amounts of raw materials used to prepare the four $Li_{1.2}Ni_{0.2}Mn_{0.6}O_2$ samples (unit mol).

Raw materials	LLO-1N1A	LLO-3N1A	LLO-4N1A	LLO-N
$LiNO_3$	0.036	0.036	0.036	0.036
$Ni(NO_3)_2·6H_2O$	0.003	0.006	0.006	0.006
$Ni(CH_3COO)_2·4H_2O$	0.003	0.000	0.000	0.000
$Mn(CH_3COO)_2·4H_2O$	0.018	0.0105	0.0084	0.000
$Mn(NO_3)_2$	0.000	0.0075	0.0096	0.018
NO_3^-/CH_3COO^- rate	1:1	3:1	4:1	4:0

Galvanostatic charge–discharge tests were performed at a LAND CT2001A battery testing system (Wuhan LAND Electronics Co., Ltd.) at room temperature between the voltage ranges of 2.0–4.8 V. Cyclic voltammetry (CV) tests of the fresh cells were performed on the ZF-100 electrochemical workstation (Shanghai Zhengfang Instruments Co., Ltd). The electrochemical impedance spectra (EIS) measurements of the cells after cycling performance test were carried out by using a CHI660D electrochemical workstation (Shanghai Chenhua Instruments Co., China). The frequency is in the range of 0.01 Hz–100 kHz with amplitude of 0.005 V.

3. Results and discussion

3.1. XRD analysis

Fig. 1 shows the XRD patterns of the four as prepared $Li_{1.2}Ni_{0.2}Mn_{0.6}O_2$ samples. The patterns were all adjusted by a Jade 6.0 soft. All their diffraction peaks can be indexed as α-$NaFeO_2$ layered structure with *R3m* space group with the additional weak broad peaks around 20–25°, which appear to consist of broadened peaks of Li_2MnO_3. The results are very record with the previous reports [15–17]. As illustrated in the Table 2, the lattice parameter, crystallite size and unit cell volume of LLO-3N1A are the smallest, in which the crystallite sizes of the four samples are calculated from XRD by a scherrer equation. This phenomenon indicates that the lattice parameter, crystallite size and unit cell volume are greatly influenced by the NO_3^-/CH_3COO^- ratio of precursors and the $Li_{1.2}Ni_{0.2}Mn_{0.6}O_2$ with smallest crystallite size of 18 nm can be obtained by choosing suitable NO_3^-/CH_3COO^- ratio of 3:1.

3.2. SEM analysis

Fig. 2 presents the SEM images of the four as prepared $Li_{1.2}Ni_{0.2}Mn_{0.6}O_2$ samples. As shown in Fig 2(a), the primary particle size of LLO-1N1A is varied from 50 nm to 300 nm. As shown in Fig. 2(b,c), nearly all the primary particle size of LLO-3N1A is about 35 nm and most of the primary particle size of LLO-4N1A is about 50 nm. As shown in Fig. 2(d), the primary particle size of LLO-N is varied from 50 nm to 150 nm and some of them are with irregular shape. Calculated the numbers of the characteristic particle sizes from Fig. 2, the average particle sizes of LLO-1N1A, LLO-3N1A, LLO-4N1A and LLO-N are illustrated in Table 3. The average primary particle size of LLO-3N1A is 35 nm, which is the smallest among the four prepared samples. The particle size analysed from SEM images also show that LLO-3N1A has

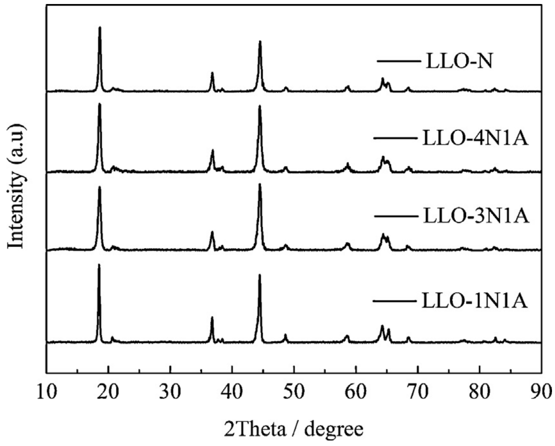

Fig. 1. XRD patterns of the four as prepared $Li_{1.2}Ni_{0.2}Mn_{0.6}O_2$ samples.